
Sparse Overlapping Sets Lasso for Multitask Learning and its Application to fMRI Analysis

Nikhil S. Rao[†]
nrao2@wisc.edu

Christopher R. Cox[#]
crrcox@wisc.edu

Robert D. Nowak[†]
nowak@ece.wisc.edu

Timothy T. Rogers[#]
ttrogers@wisc.edu

[†] Department of Electrical and Computer Engineering, [#] Department of Psychology
University of Wisconsin- Madison

Abstract

Multitask learning can be effective when features useful in one task are also useful for other tasks, and the group lasso is a standard method for selecting a common subset of features. In this paper, we are interested in a less restrictive form of multitask learning, wherein (1) the available features can be organized into subsets according to a notion of similarity and (2) features useful in one task are similar, but not necessarily identical, to the features best suited for other tasks. The main contribution of this paper is a new procedure called *Sparse Overlapping Sets (SOS) lasso*, a convex optimization that automatically selects similar features for related learning tasks. Error bounds are derived for SOSlasso and its consistency is established for squared error loss. In particular, SOSlasso is motivated by multi-subject fMRI studies in which functional activity is classified using brain voxels as features. Experiments with real and synthetic data demonstrate the advantages of SOSlasso compared to the lasso and group lasso.

1 Introduction

Multitask learning exploits the relationships between several learning tasks in order to improve performance, which is especially useful if a common subset of features are useful for all tasks at hand. The group lasso (Glasso) [21, 10] is naturally suited for this situation: if a feature is selected for one task, then it is selected for all tasks. This may be too restrictive in many applications, and this motivates a less rigid approach to multitask feature selection. Suppose that the available features can be organized into overlapping subsets according to a notion of similarity, and that the features useful in one task are similar, but not necessarily identical, to those best suited for other tasks. In other words, a feature that is useful for one task suggests that the subset it belongs to may contain the features useful in other tasks (Figure 1).

In this paper, we introduce the *sparse overlapping sets lasso* (SOSlasso), a convex program to recover the sparsity patterns corresponding to the situations explained above. SOSlasso generalizes lasso [18] and Glasso, effectively spanning the range between these two well-known procedures. SOSlasso is capable of exploiting the similarities between useful features across tasks, but unlike Glasso it does not force different tasks to use exactly the same features. It produces sparse solutions, but unlike lasso it encourages similar patterns of sparsity across tasks. Sparse group lasso [16] is a special case of SOSlasso that only applies to disjoint sets, a significant limitation when features cannot be easily partitioned, as is the case of our motivating example in fMRI. The main contribution of this paper is a theoretical analysis of SOSlasso, which also covers sparse group lasso as a special case (further differentiating us from [16]). The performance of SOSlasso is analyzed, error

bounds are derived for general loss functions, and its consistency is shown for squared error loss. Experiments with real and synthetic data demonstrate the advantages of SOSlasso relative to lasso and Glasso.

1.1 Sparse Overlapping Sets

SOSlasso encourages sparsity patterns that are similar, but not identical, across tasks. This is accomplished by decomposing the features of each task into groups $G_1 \dots G_M$, where M is the same for each task, and G_i is a set of features that can be considered similar across tasks. Conceptually, SOSlasso first selects subsets that are most useful for all tasks, and then identifies a unique sparse solution for each task drawing only from features in the selected subsets. In the fMRI application discussed later, the subsets are simply clusters of adjacent spatial data points (voxels) in the brains of multiple subjects. Figure 1 shows an example of the patterns that typically arise in sparse multitask learning applications, where rows indicate features and columns correspond to tasks.

Past work has focused on recovering variables that exhibit within and across group sparsity, when the groups do not overlap [16], finding application in genetics, handwritten character recognition [17] and climate and oceanography [2]. Along related lines, the exclusive lasso [23] can be used when it is explicitly known that variables in certain sets are negatively correlated.

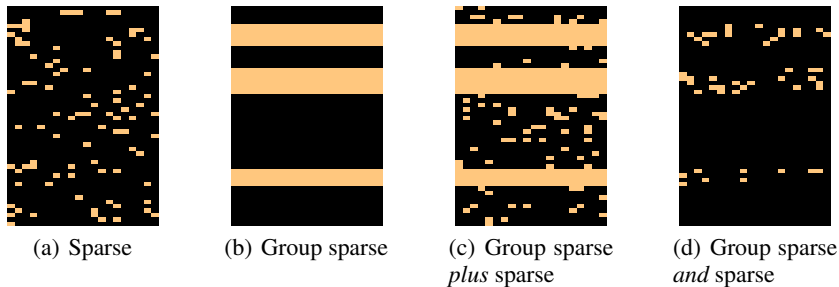


Figure 1: A comparison of different sparsity patterns. (a) shows a standard sparsity pattern. An example of group sparse patterns promoted by Glasso [21] is shown in (b). In (c), we show the patterns considered in [7]. Finally, in (d), we show the patterns we are interested in this paper.

1.2 fMRI Applications

In psychological studies involving fMRI, multiple participants are scanned while subjected to exactly the same experimental manipulations. Cognitive Neuroscientists are interested in identifying the patterns of activity associated with different cognitive states, and construct a model of the activity that accurately predicts the cognitive state evoked on novel trials. In these datasets, it is reasonable to expect that the same general areas of the brain will respond to the manipulation in every participant. However, the specific patterns of activity in these regions will vary, both because neural codes can vary by participant [4] and because brains vary in size and shape, rendering neuroanatomy only an approximate guide to the location of relevant information across individuals. In short, a voxel useful for prediction in one participant suggests the general anatomical neighborhood where useful voxels may be found, but not the precise voxel. While logistic Glasso [19], lasso [15], and the elastic net penalty [14] have been applied to neuroimaging data, these methods do not exclusively take into account both the common macrostructure and the differences in microstructure across brains. SOSlasso, in contrast, lends itself well to such a scenario, as we will see from our experiments.

1.3 Organization

The rest of the paper is organized as follows: in Section 2, we outline the notations that we will use and formally set up the problem. We also introduce the SOSlasso regularizer. We derive certain key properties of the regularizer in Section 3. In Section 4, we specialize the problem to the multitask linear regression setting (2), and derive consistency rates for the same, leveraging ideas from [11]. We outline experiments performed on simulated data in Section 5. In this section, we also perform logistic regression on fMRI data, and argue that the use of the SOSlasso yields interpretable multivariate solutions compared to Glasso and lasso.

2 Sparse Overlapping Sets Lasso

We formalize the notations used in the sequel. Lowercase and uppercase bold letters indicate vectors and matrices respectively. We assume a multitask learning framework, with a data matrix $\Phi_t \in \mathbb{R}^{n \times p}$ for each task $t \in \{1, 2, \dots, \mathcal{T}\}$. We assume there exists a vector $\mathbf{x}_t^* \in \mathbb{R}^p$ such that measurements obtained are of the form $\mathbf{y}_t = \Phi_t \mathbf{x}_t^* + \eta_t$ $\eta_t \sim \mathcal{N}(0, \sigma^2 \mathbf{I})$. Let $\mathbf{X}^* := [\mathbf{x}_1^* \ \mathbf{x}_2^* \ \dots \ \mathbf{x}_T^*] \in \mathbb{R}^{p \times \mathcal{T}}$. Suppose we are given M (possibly overlapping) groups $\tilde{\mathcal{G}} = \{\tilde{G}_1, \tilde{G}_2, \dots, \tilde{G}_M\}$, so that $\tilde{G}_i \subset \{1, 2, \dots, p\} \ \forall i$, of maximum size B . These groups contain sets of ‘‘similar’’ features, the notion of similarity being application dependent. We assume that all but $k \ll M$ groups are identically zero. Among the active groups, we further assume that at most only a fraction $\alpha \in (0, 1)$ of the coefficients per group are non zero. We consider the following optimization program in this paper

$$\hat{\mathbf{X}} = \arg \min_{\mathbf{x}} \left\{ \sum_{t=1}^{\mathcal{T}} \mathcal{L}_{\Phi_t}(\mathbf{x}_t) + \lambda_n h(\mathbf{x}) \right\} \quad (1)$$

where $\mathbf{x} = [\mathbf{x}_1^T \ \mathbf{x}_2^T \ \dots \ \mathbf{x}_T^T]^T$, $h(\mathbf{x})$ is a regularizer and $\mathcal{L}_t := \mathcal{L}_{\Phi_t}(\mathbf{x}_t)$ denotes the loss function, whose value depends on the data matrix Φ_t . We consider least squares and logistic loss functions. In the least squares setting, we have $\mathcal{L}_t = \frac{1}{2n} \|\mathbf{y}_t - \Phi_t \mathbf{x}_t\|^2$. We reformulate the optimization problem (1) with the least squares loss as

$$\hat{\mathbf{x}} = \arg \min_{\mathbf{x}} \left\{ \frac{1}{2n} \|\mathbf{y} - \Phi \mathbf{x}\|_2^2 + \lambda_n h(\mathbf{x}) \right\} \quad (2)$$

where $\mathbf{y} = [\mathbf{y}_1^T \ \mathbf{y}_2^T \ \dots \ \mathbf{y}_T^T]^T$ and the block diagonal matrix Φ is formed by block concatenating the Φ_t 's. We use this reformulation for ease of exposition (see also [10] and references therein). Note that $\mathbf{x} \in \mathbb{R}^{Tp}$, $\mathbf{y} \in \mathbb{R}^{Tn}$, and $\Phi \in \mathbb{R}^{Tn \times Tp}$. We also define $\mathcal{G} = \{G_1, G_2, \dots, G_M\}$ to be the set of groups defined on \mathbb{R}^{Tp} formed by aggregating the rows of \mathbf{X} that were originally in $\tilde{\mathcal{G}}$, so that \mathbf{x} is composed of groups $G \in \mathcal{G}$.

We next define a regularizer h that promotes sparsity both within and across overlapping sets of similar features:

$$h(\mathbf{x}) = \inf_{\mathcal{W}} \sum_{G \in \mathcal{G}} (\alpha_G \|\mathbf{w}_G\|_2 + \|\mathbf{w}_G\|_1) \quad \text{s.t.} \quad \sum_{G \in \mathcal{G}} \mathbf{w}_G = \mathbf{x} \quad (3)$$

where the $\alpha_G > 0$ are constants that balance the tradeoff between the group norms and the ℓ_1 norm. Each \mathbf{w}_G has the same size as \mathbf{x} , with support restricted to the variables indexed by group G . \mathcal{W} is a set of vectors, where each vector has a support restricted to one of the groups $G \in \mathcal{G}$:

$$\mathcal{W} = \{\mathbf{w}_G \in \mathbb{R}^{Tp} \mid [\mathbf{w}_G]_i = 0 \text{ if } i \notin G\}$$

where $[\mathbf{w}_G]_i$ is the i^{th} coefficient of \mathbf{w}_G . The *SOSlasso* is the optimization in (1) with $h(\mathbf{x})$ as defined in (3).

We say the set of vectors \mathbf{w}_G is an optimal decomposition of \mathbf{x} if they achieve the inf in (3). The objective function in (3) is convex and coercive. Hence, $\forall \mathbf{x}$, an optimal decomposition always exists.

As the $\alpha_G \rightarrow \infty$ the ℓ_1 term becomes redundant, reducing $h(\mathbf{x})$ to the overlapping group lasso penalty introduced in [6], and studied in [12, 13]. When the $\alpha_G \rightarrow 0$, the overlapping group lasso term vanishes and $h(\mathbf{x})$ reduces to the lasso penalty. We consider $\alpha_G = 1 \ \forall G$. All the results in the paper can be easily modified to incorporate different settings for the α_G .

Support	Values	$\sum_G \ \mathbf{x}_G\ _2$	$\ \mathbf{x}\ _1$	$\sum_G (\ \mathbf{x}_G\ _2 + \ \mathbf{x}_G\ _1)$
{1, 4, 9}	{3, 4, 7}	12	14	26
{1, 2, 3, 4, 5}	{2, 5, 2, 4, 5}	8.602	18	26.602
{1, 3, 4}	{3, 4, 7}	8.602	14	22.602

Table 1: Different instances of a 10-d vector and their corresponding norms.

The example in Table 1 gives an insight into the kind of sparsity patterns preferred by the function $h(\mathbf{x})$. The optimization problems (1) and (2) will prefer solutions that have a small value of $h(\cdot)$.

Consider 3 instances of $\mathbf{x} \in \mathbb{R}^{10}$, and the corresponding group lasso, ℓ_1 , and $h(\mathbf{x})$ function values. The vector is assumed to be made up of two groups, $G_1 = \{1, 2, 3, 4, 5\}$ and $G_2 = \{6, 7, 8, 9, 10\}$. $h(\mathbf{x})$ is smallest when the support set is sparse within groups, and also when only one of the two groups is selected. The ℓ_1 norm does not take into account sparsity across groups, while the group lasso norm does not take into account sparsity within groups.

To solve (1) and (2) with the regularizer proposed in (3), we use the covariate duplication method of [6], to reduce the problem to a non overlapping sparse group lasso problem. We then use proximal point methods [8] in conjunction with the MALSAR [22] package to solve the optimization problem.

3 Error Bounds for SOSlasso with General Loss Functions

We derive certain key properties of the regularizer $h(\cdot)$ in (3), independent of the loss function used.

Lemma 3.1 *The function $h(\mathbf{x})$ in (3) is a norm*

The proof follows from basic properties of norms and because if $\mathbf{w}_G, \mathbf{v}_G$ are optimal decompositions of \mathbf{x}, \mathbf{y} , then it does not imply that $\mathbf{w}_G + \mathbf{v}_G$ is an optimal decomposition of $\mathbf{x} + \mathbf{y}$. For a detailed proof, please refer to the supplementary material.

The dual norm of $h(\mathbf{x})$ can be bounded as

$$\begin{aligned}
h^*(\mathbf{u}) &= \max_{\mathbf{x}} \{\mathbf{x}^T \mathbf{u}\} \text{ s.t. } h(\mathbf{x}) \leq 1 \\
&= \max_{\mathcal{W}} \left\{ \sum_{G \in \mathcal{G}} \mathbf{w}_G^T \mathbf{u}_G \right\} \text{ s.t. } \sum_{G \in \mathcal{G}} (\|\mathbf{w}_G\|_2 + \|\mathbf{w}_G\|_1) \leq 1 \\
&\stackrel{(i)}{\leq} \max_{\mathcal{W}} \left\{ \sum_{G \in \mathcal{G}} \mathbf{w}_G^T \mathbf{u}_G \right\} \text{ s.t. } \sum_{G \in \mathcal{G}} 2\|\mathbf{w}_G\|_2 \leq 1 \\
&= \max_{\mathcal{W}} \left\{ \sum_{G \in \mathcal{G}} \mathbf{w}_G^T \mathbf{u}_G \right\} \text{ s.t. } \sum_{G \in \mathcal{G}} \|\mathbf{w}_G\|_2 \leq \frac{1}{2} \\
\Rightarrow h^*(\mathbf{u}) &\leq \max_{G \in \mathcal{G}} \frac{1}{2} \|\mathbf{u}_G\|_2 \tag{4}
\end{aligned}$$

(i) follows from the fact that the constraint set in (i) is a superset of the constraint set in the previous statement, since $\|\mathbf{a}\|_2 \leq \|\mathbf{a}\|_1$. (4) follows from noting that the maximum is obtained by setting $\mathbf{w}_{G^*} = \frac{\mathbf{u}_{G^*}}{2\|\mathbf{u}_{G^*}\|_2}$, where $G^* = \arg \max_{G \in \mathcal{G}} \|\mathbf{u}_G\|_2$. The inequality (4) is far more tractable than the actual dual norm, and will be useful in our derivations below. Since $h(\cdot)$ is a norm, we can apply methods developed in [11] to derive consistency rates for the optimization problems (1) and (2). We will use the same notations as in [11] wherever possible.

Definition 3.2 *A norm $h(\cdot)$ is decomposable with respect to the subspace pair $sA \subset sB$ if $h(\mathbf{a} + \mathbf{b}) = h(\mathbf{a}) + h(\mathbf{b}) \forall \mathbf{a} \in sA, \mathbf{b} \in sB^\perp$.*

Lemma 3.3 *Let $\mathbf{x}^* \in \mathbb{R}^p$ be a vector that can be decomposed into (overlapping) groups with within-group sparsity. Let $\mathcal{G}^* \subset \mathcal{G}$ be the set of active groups of \mathbf{x}^* . Let $S = \text{supp}(\mathbf{x}^*)$ indicate the support set of \mathbf{x} . Let sA be the subspace spanned by the coordinates indexed by S , and let $sB = sA$. We then have that the norm in (3) is decomposable with respect to sA, sB*

The result follows in a straightforward way from noting that supports of decompositions for vectors in sA and sB^\perp do not overlap. We defer the proof to the supplementary material.

Definition 3.4 *Given a subspace sB , the subspace compatibility constant with respect to a norm $\|\cdot\|$ is given by*

$$\Psi(B) = \sup \left\{ \frac{h(\mathbf{x})}{\|\mathbf{x}\|} \mid \forall \mathbf{x} \in sB \setminus \{\mathbf{0}\} \right\}$$

Lemma 3.5 *Consider a vector \mathbf{x} that can be decomposed into $\mathcal{G}^* \subset \mathcal{G}$ active groups. Suppose the maximum group size is B , and also assume that a fraction $\alpha \in (0, 1)$ of the coordinates in each active group is non zero. Then,*

$$h(\mathbf{x}) \leq (1 + \sqrt{B\alpha}) \sqrt{|\mathcal{G}^*|} \|\mathbf{x}\|_2$$

Proof For any vector \mathbf{x} with $\text{supp}(\mathbf{x}) \subset \mathcal{G}^*$, there exists a representation $\mathbf{x} = \sum_{G \in \mathcal{G}^*} \mathbf{w}_G$, such that the supports of the different \mathbf{w}_G do not overlap. Then,

$$h(\mathbf{x}) \leq \sum_{G \in \mathcal{G}^*} (\|\mathbf{w}_G\|_2 + \|\mathbf{w}_G\|_1) \leq (1 + \sqrt{B\alpha}) \sum_{G \in \mathcal{G}^*} \|\mathbf{w}_G\|_2 \leq (1 + \sqrt{B\alpha}) \sqrt{|\mathcal{G}^*|} \|\mathbf{x}\|_2$$

■

We see that $(1 + \sqrt{B\alpha}) \sqrt{|\mathcal{G}^*|}$ (Lemma 3.5) gives an upper bound on the subspace compatibility constant with respect to the ℓ_2 norm for the subspace indexed by the support of the vector, which is contained in the span of the union of groups in \mathcal{G}^* .

Definition 3.6 For a given set S , and given vector \mathbf{x}^* , the loss function $\mathcal{L}_{\Phi}(\mathbf{x})$ satisfies the Restricted Strong Convexity (RSC) condition with parameter κ and tolerance τ if

$$\mathcal{L}_{\Phi}(\mathbf{x}^* + \Delta) - \mathcal{L}_{\Phi}(\mathbf{x}^*) - \langle \nabla \mathcal{L}_{\Phi}(\mathbf{x}^*), \Delta \rangle \geq \kappa \|\Delta\|_2^2 - \tau^2(\mathbf{x}^*) \quad \forall \Delta \in S$$

In this paper, we consider vectors \mathbf{x}^* that lie exactly in $k \ll M$ groups, and display within-group sparsity. This implies that the tolerance $\tau(\mathbf{x}^*) = 0$, and we will ignore this term henceforth.

We also define the following set, which will be used in the sequel:

$$C(sA, sB, \mathbf{x}^*) := \{\Delta \in \mathbb{R}^p \mid h(\Pi_{sB^\perp} \Delta) \leq 3h(\Pi_{sB} \Delta) + 4h(\Pi_{sA^\perp} \mathbf{x}^*)\} \quad (5)$$

where $\Pi_{sA}(\cdot)$ denotes the projection onto the subspace sA . Based on the results above, we can now apply a result from [11] to the SOSlasso:

Theorem 3.7 (Corollary 1 in [11]) Consider a convex and differentiable loss function such that RSC holds with constants κ and $\tau = 0$ over (5), and a norm $h(\cdot)$ decomposable over sets sA and sB . For the optimization program in (1), using the parameter $\lambda_n \geq 2h^*(\nabla \mathcal{L}_{\Phi}(\mathbf{x}^*))$, any optimal solution $\hat{\mathbf{x}}_{\lambda_n}$ to (1) satisfies

$$\|\hat{\mathbf{x}}_{\lambda_n} - \mathbf{x}^*\|_2^2 \leq \frac{9\lambda_n^2}{\kappa} \Psi^2(sB)$$

The result above shows a general bound on the error using the lasso with sparse overlapping sets. Note that the regularization parameter λ_n as well as the RSC constant κ depend on the loss function $\mathcal{L}_{\Phi}(\mathbf{x})$. Convergence for logistic regression settings may be derived using methods in [1]. In the next section, we consider the least squares loss (2), and show that the estimate using the SOSlasso is consistent.

4 Consistency of SOSlasso with Squared Error Loss

We first need to bound the dual norm of the gradient of the loss function, so as to bound λ_n . Consider $\mathcal{L} := \mathcal{L}_{\Phi}(\mathbf{x}) = \frac{1}{2n} \|\mathbf{y} - \Phi \mathbf{x}\|^2$. The gradient of the loss function with respect to \mathbf{x} is given by $\nabla \mathcal{L} = \frac{1}{n} \Phi^T (\Phi \mathbf{x} - \mathbf{y}) = \frac{1}{n} \Phi^T \eta$ where $\eta = [\eta_1^T \eta_2^T \dots \eta_T^T]^T$ (see Section 2). Our goal now is to find an upper bound on the quantity $h^*(\nabla \mathcal{L})$, which from (4) is

$$\frac{1}{2} \max_{G \in \mathcal{G}} \|\nabla \mathcal{L}_G\|_2 = \frac{1}{2n} \max_{G \in \mathcal{G}} \|\Phi_G^T \eta\|_2$$

where Φ_G is the matrix Φ restricted to the columns indexed by the group G . We will prove an upper bound for the above quantity in the course of the results that follow.

Since $\eta \sim \mathcal{N}(0, \sigma^2 \mathbf{I})$, we have $\Phi_G^T \eta \sim \sigma \mathcal{N}(0, \Phi_G^T \Phi_G)$. Defining $\sigma_{mG} := \sigma_{\max}\{\Phi_G^T \Phi_G\}$ to be the maximum singular value, we have $\|\Phi_G^T \eta\|_2^2 \leq \sigma^2 \sigma_{mG}^2 \|\gamma\|_2^2$, where $\gamma \sim \mathcal{N}(0, \mathbf{I}_{|G|}) \Rightarrow \|\gamma\|_2^2 \sim \chi_{|G|}^2$, where χ_d^2 is a chi-squared random variable with d degrees of freedom. This allows us to work with the more tractable chi squared random variable when we look to bound the dual norm of $\nabla \mathcal{L}$. The next lemma helps us obtain a bound on the maximum of χ^2 random variables.

Lemma 4.1 Let z_1, z_2, \dots, z_M be chi-squared random variables with d degrees of freedom. Then for some constant c ,

$$\mathbb{P} \left(\max_{i=1,2,\dots,M} z_i \leq c^2 d \right) \geq 1 - \exp \left(\log(M) - \frac{(c-1)^2 d}{2} \right)$$

Proof From the chi-squared tail bound in [3], $\mathbb{P}(z_i \geq c^2 d) \leq \exp\left(-\frac{(c-1)^2 d}{2}\right)$. The result follows from a union bound and inverting the expression. \blacksquare

Lemma 4.2 Consider the loss function $\mathcal{L} := \frac{1}{2n} \sum_{t=1}^{\mathcal{T}} \|\mathbf{y}_t - \Phi_t \mathbf{x}_t\|^2 = \frac{1}{2n} \|\mathbf{y} - \Phi \mathbf{x}\|^2$, with the Φ_t 's deterministic and the measurements corrupted with AWGN of variance σ^2 . For the regularizer in (3), the dual norm of the gradient of the loss function is bounded as

$$h^*(\nabla \mathcal{L})^2 \leq \frac{\sigma^2 \sigma_m^2 (\log(M) + \mathcal{T}B)}{4n}$$

with probability at least $1 - c_1 \exp(-c_2 n)$, for $c_1, c_2 > 0$, and where $\sigma_m = \max_{G \in \mathcal{G}} \sigma_{mG}$

Proof Let $\gamma \sim \chi_{\mathcal{T}|G|}^2$. We begin with the upper bound obtained for the dual norm of the regularizer in (4):

$$\begin{aligned} h^*(\nabla \mathcal{L})^2 &\stackrel{(i)}{\leq} \frac{1}{4} \max_{G \in \mathcal{G}} \left\| \frac{1}{n} \Phi_G^T \eta \right\|_2^2 \leq \frac{\sigma^2}{4} \max_{G \in \mathcal{G}} \frac{\sigma_{mG}^2 \gamma}{n^2} \\ &\stackrel{(ii)}{\leq} \frac{\sigma^2 \sigma_m^2}{4} \max_{G \in \mathcal{G}} \frac{\gamma}{n^2} \stackrel{(iii)}{\leq} \frac{\sigma^2 \sigma_m^2}{4} c^2 \mathcal{T}B \quad \mathbf{w. p.} \ 1 - \exp\left(\log(M) - \frac{(cn-1)^2 \mathcal{T}B}{2}\right) \end{aligned}$$

where (i) follows from the formulation of the gradient of the loss function and the fact that the square of maximum of non negative numbers is the maximum of the squares of the same numbers. In (ii), we have defined $\sigma_m = \max_G \sigma_{mG}$. Finally, we have made use of Lemma 4.1 in (iii). We then set

$$c^2 = \frac{\log(M) + \mathcal{T}B}{\mathcal{T}Bn}$$

to obtain the result. \blacksquare

We combine the results developed so far to derive the following consistency result for the SOS lasso, with the least squares loss function.

Theorem 4.3 Suppose we obtain linear measurements of a sparse overlapping grouped matrix $\mathbf{X}^* \in \mathbb{R}^{p \times \mathcal{T}}$, corrupted by AWGN of variance σ^2 . Suppose the matrix \mathbf{X}^* can be decomposed into M possible overlapping groups of maximum size B , out of which k are active. Furthermore, assume that a fraction $\alpha \in (0, 1]$ of the coefficients are non zero in each active group. Consider the following vectorized SOSlasso multitask regression problem (2):

$$\begin{aligned} \hat{\mathbf{x}} &= \arg \min_{\mathbf{x}} \left\{ \frac{1}{2n} \|\mathbf{y} - \Phi \mathbf{x}\|_2^2 + \lambda_n h(\mathbf{x}) \right\}, \\ h(\mathbf{x}) &= \inf_{\mathcal{W}} \sum_{G \in \mathcal{G}} (\|\mathbf{w}_G\|_2 + \|\mathbf{w}_G\|_1) \quad \mathbf{s.t.} \quad \sum_{G \in \mathcal{G}} \mathbf{w}_G = \mathbf{x} \end{aligned}$$

Suppose the data matrices Φ_t are non random, and the loss function satisfies restricted strong convexity assumptions with parameter κ . Then, for $\lambda_n^2 \geq \frac{\sigma^2 \sigma_m^2 (\log(M) + \mathcal{T}B)}{4n}$, the following holds with probability at least $1 - c_1 \exp(-c_2 n)$, with $c_1, c_2 > 0$:

$$\|\hat{\mathbf{x}} - \mathbf{x}^*\|_2^2 \leq \frac{9 \sigma^2 \sigma_m^2 \left(1 + \sqrt{\mathcal{T}B\alpha}\right)^2 k (\log(M) + \mathcal{T}B)}{4n\kappa}$$

where we define $\sigma_m := \max_{G \in \mathcal{G}} \sigma_{\max}\{\Phi_G^T \Phi_G\}$

Proof Follows from substituting in Theorem 3.7 the results from Lemma 3.5 and Lemma 4.2. \blacksquare

From [11], we see that the convergence rate matches that of the group lasso, with an additional multiplicative factor α . This stems from the fact that the signal has a sparse structure ‘‘embedded’’ within a group sparse structure. Visualizing the optimization problem as that of solving a lasso within a group lasso framework lends some intuition into this result. Note that since $\alpha < 1$, this bound is much smaller than that of the standard group lasso.

5 Experiments and Results

5.1 Synthetic data, Gaussian Linear Regression

For $\mathcal{T} = 20$ tasks, we define a $N = 2002$ element vector divided into $M = 500$ groups of size $B = 6$. Each group overlaps with its neighboring groups ($G_1 = \{1, 2, \dots, 6\}$, $G_2 = \{5, 6, \dots, 10\}$, $G_3 = \{9, 10, \dots, 14\}, \dots$). 20 of these groups were activated uniformly at random, and populated from a uniform $[-1, 1]$ distribution. A proportion α of these coefficients with largest magnitude were retained as true signal. For each task, we obtain 250 linear measurements using a $\mathcal{N}(0, \frac{1}{250}\mathbf{I})$ matrix. We then corrupt each measurement with Additive White Gaussian Noise (AWGN), and assess signal recovery in terms of Mean Squared Error (MSE). The regularization parameter was clairvoyantly picked to minimize the MSE over a range of parameter values. The results of applying lasso, standard latent group lasso [6, 12], and our SOSlasso to these data are plotted in Figures 2(a), varying σ , $\alpha = 0.2$, and 2(b), varying α , $\sigma = 0.1$. Each point in Figures 2(a) and 2(b), is the average of 100 trials, where each trial is based on a new random instance of \mathbf{X}^* and the Gaussian data matrices.

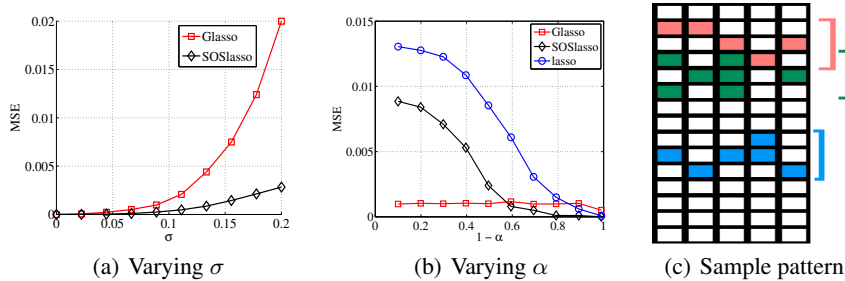


Figure 2: As the noise is increased (a), our proposed penalty function (SOSlasso) allows us to recover the true coefficients more accurately than the group lasso (Glasso). Also, when alpha is large, the active groups are not sparse, and the standard overlapping group lasso outperforms the other methods. However, as α reduces, the method we propose outperforms the group lasso (b). (c) shows a toy sparsity pattern, with different colors denoting different overlapping groups

5.2 The SOSlasso for fMRI

In this experiment, we compared SOSlasso, lasso, and Glasso in analysis of the star-plus dataset [20]. 6 subjects made judgements that involved processing 40 sentences and 40 pictures while their brains were scanned in half second intervals using fMRI¹. We retained the 16 time points following each stimulus, yielding 1280 measurements at each voxel. The task is to distinguish, at each point in time, which stimulus a subject was processing. [20] showed that there exists cross-subject consistency in the cortical regions useful for prediction in this task. Specifically, experts partitioned each dataset into 24 non overlapping regions of interest (ROIs), then reduced the data by discarding all but 7 ROIs and, for each subject, averaging the BOLD response across voxels within each ROI and showed that a classifier trained on data from 5 subjects generalized when applied to data from a 6th.

We assessed whether SOSlasso could leverage this cross-individual consistency to aid in the discovery of predictive voxels without requiring expert pre-selection of ROIs, or data reduction, or any alignment of voxels beyond that existing in the raw data. Note that, unlike [20], we do not aim to learn a solution that generalizes to a withheld subject. Rather, we aim to discover a group sparsity pattern that suggests a similar set of voxels in all subjects, before optimizing a separate solution for each individual. If SOSlasso can exploit cross-individual anatomical similarity from this raw, coarsely-aligned data, it should show reduced cross-validation error relative to the lasso applied separately to each individual. If the solution is sparse within groups and highly variable across individuals, SOSlasso should show reduced cross-validation error relative to Glasso. Finally, if SOSlasso is finding useful cross-individual structure, the features it selects should align at least somewhat with the expert-identified ROIs shown by [20] to carry consistent information.

¹Data and documentation available at <http://www.cs.cmu.edu/afs/cs.cmu.edu/project/theo-81/www/>

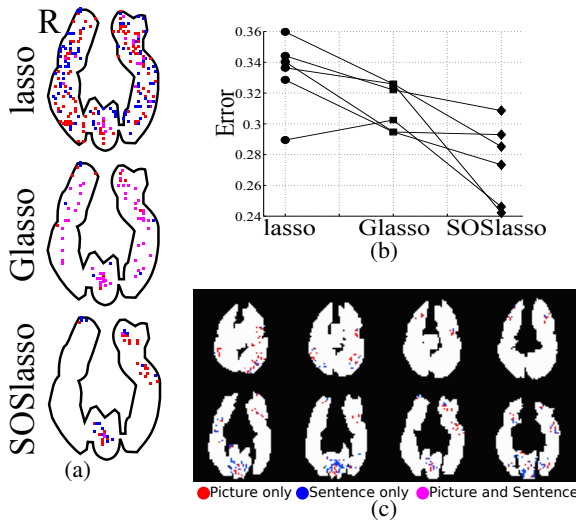


Figure 3: Results from fMRI experiments. (a) Aggregated sparsity patterns for a single brain slice. (b) Cross-validation error obtained with each method. Lines connect data for a single subject. (c) The full sparsity pattern obtained with SOSlasso.

Method	% ROI	t(5), p
lasso	46.11	6.08 ,0.001
Glasso	50.89	5.65 ,0.002
SOSlasso	70.31	

Table 2: Proportion of selected voxels in the 7 relevant ROIs aggregated over subjects, and corresponding two-tailed significance levels for the contrast of lasso and Glasso to SOSlasso.

We trained 3 classifiers using 4-fold cross validation to select the regularization parameter, considering all available voxels without preselection. We group regions of $5 \times 5 \times 1$ voxels and considered overlapping groups “shifted” by 2 voxels in the first 2 dimensions.² Figure 3(b) shows the individual error rates across the 6 subjects for the three methods. Across subjects, SOSlasso had a significantly lower cross-validation error rate (27.47 %) than individual lasso (33.3 %; within-subjects $t(5) = 4.8$; $p = 0.004$ two-tailed), showing that the method can exploit anatomical similarity across subjects to learn a better classifier for each. SOSlasso also showed significantly lower error rates than glasso (31.1 %; $t(5) = 2.92$; $p = 0.03$ two-tailed), suggesting that the signal is sparse within selected regions and variable across subjects.

Figure 3(a) presents a sample of the the sparsity patterns obtained from the different methods, aggregated over all subjects. Red points indicate voxels that contributed positively to picture classification in at least one subject, but never to sentences; Blue points have the opposite interpretation. Purple points indicate voxels that contributed positively to picture and sentence classification in different subjects. The remaining slices for the SOSlasso are shown in Figure 3(c). There are three things to note from Figure 3(a). First, the Glasso solution is fairly dense, with many voxels signaling both picture and sentence across subjects. We believe this “purple haze” demonstrates why Glasso is ill-suited for fMRI analysis: a voxel selected for one subject must also be selected for all others. This approach will not succeed if, as is likely, there exists no direct voxel-to-voxel correspondence or if the neural code is variable across subjects. Second, the lasso solution is less sparse than the SOSlasso because it allows any task-correlated voxel to be selected. It leads to a higher cross-validation error, indicating that the ungrouped voxels are inferior predictors (Figure 3(b)). Third, the SOSlasso not only yields a sparse solution, but also clustered. To assess how well these clusters align with the anatomical regions thought *a-priori* to be involved in sentence and picture representation, we calculated the proportion of selected voxels falling within the 7 ROIs identified by [20] as relevant to the classification task (Table 2). For SOSlasso an average of 70% of identified voxels fell within these ROIs, significantly more than for lasso or Glasso.

6 Conclusions and Extensions

We have introduced SOSlasso, a function that recovers sparsity patterns that are a hybrid of overlapping group sparse and sparse patterns when used as a regularizer in convex programs, and proved its theoretical convergence rates when minimizing least squares. The SOSlasso succeeds in a multi-task fMRI analysis, where it both makes better inferences and discovers more theoretically plausible brain regions that lasso and Glasso. Future work involves experimenting with different parameters for the group and l1 penalties, and using other similarity groupings, such as functional connectivity in fMRI.

²The irregular group size compensates for voxels being larger and scanner coverage being smaller in the z-dimension (only 8 slices relative to 64 in the x- and y-dimensions).

References

- [1] Francis Bach. Adaptivity of averaged stochastic gradient descent to local strong convexity for logistic regression. *arXiv preprint arXiv:1303.6149*, 2013.
- [2] S. Chatterjee, A. Banerjee, and A. Ganguly. Sparse group lasso for regression on land climate variables. In *Data Mining Workshops (ICDMW), 2011 IEEE 11th International Conference on*, pages 1–8. IEEE, 2011.
- [3] S. Dasgupta, D. Hsu, and N. Verma. A concentration theorem for projections. *arXiv preprint arXiv:1206.6813*, 2012.
- [4] Eva Feredoes, Giulio Tononi, and Bradley R Postle. The neural bases of the short-term storage of verbal information are anatomically variable across individuals. *The Journal of Neuroscience*, 27(41):11003–11008, 2007.
- [5] James V Haxby, M Ida Gobbini, Maura L Furey, Alumit Ishai, Jennifer L Schouten, and Pietro Pietrini. Distributed and overlapping representations of faces and objects in ventral temporal cortex. *Science*, 293(5539):2425–2430, 2001.
- [6] L. Jacob, G. Obozinski, and J. P. Vert. Group lasso with overlap and graph lasso. In *Proceedings of the 26th Annual International Conference on Machine Learning*, pages 433–440. ACM, 2009.
- [7] A. Jalali, P. Ravikumar, S. Sanghavi, and C. Ruan. A dirty model for multi-task learning. *Advances in Neural Information Processing Systems*, 23:964–972, 2010.
- [8] R. Jenatton, J. Mairal, G. Obozinski, and F. Bach. Proximal methods for hierarchical sparse coding. *arXiv preprint arXiv:1009.2139*, 2010.
- [9] Rodolphe Jenatton, Alexandre Gramfort, Vincent Michel, Guillaume Obozinski, Evelyn Eger, Francis Bach, and Bertrand Thirion. Multiscale mining of fmri data with hierarchical structured sparsity. *SIAM Journal on Imaging Sciences*, 5(3):835–856, 2012.
- [10] K. Lounici, M. Pontil, A. B. Tsybakov, and S. van de Geer. Taking advantage of sparsity in multi-task learning. *arXiv preprint arXiv:0903.1468*, 2009.
- [11] S. N. Negahban, P. Ravikumar, M. J Wainwright, and Bin Yu. A unified framework for high-dimensional analysis of m -estimators with decomposable regularizers. *Statistical Science*, 27(4):538–557, 2012.
- [12] G. Obozinski, L. Jacob, and J.P. Vert. Group lasso with overlaps: The latent group lasso approach. *arXiv preprint arXiv:1110.0413*, 2011.
- [13] N. Rao, B. Recht, and R. Nowak. Universal measurement bounds for structured sparse signal recovery. In *Proceedings of AISTATS*, volume 2102, 2012.
- [14] Irina Rish, Guillermo A Cecchia, Kyle Heutonb, Marwan N Balikic, and A Vania Apkarianc. Sparse regression analysis of task-relevant information distribution in the brain. In *Proceedings of SPIE*, volume 8314, page 831412, 2012.
- [15] Srikanth Ryali, Kaustubh Supekar, Daniel A Abrams, and Vinod Menon. Sparse logistic regression for whole brain classification of fmri data. *NeuroImage*, 51(2):752, 2010.
- [16] N. Simon, J. Friedman, T. Hastie, and R. Tibshirani. A sparse-group lasso. *Journal of Computational and Graphical Statistics*, (just-accepted), 2012.
- [17] P. Sprechmann, I. Ramirez, G. Sapiro, and Y. Eldar. Collaborative hierarchical sparse modeling. In *Information Sciences and Systems (CISS), 2010 44th Annual Conference on*, pages 1–6. IEEE, 2010.
- [18] Robert Tibshirani. Regression shrinkage and selection via the lasso. *Journal of the Royal Statistical Society. Series B (Methodological)*, pages 267–288, 1996.
- [19] Marcel van Gerven, Christian Hesse, Ole Jensen, and Tom Heskes. Interpreting single trial data using groupwise regularisation. *NeuroImage*, 46(3):665–676, 2009.
- [20] X. Wang, T. M Mitchell, and R. Hutchinson. Using machine learning to detect cognitive states across multiple subjects. *CALD KDD project paper*, 2003.
- [21] M. Yuan and Y. Lin. Model selection and estimation in regression with grouped variables. *Journal of the Royal Statistical Society: Series B (Statistical Methodology)*, 68(1):49–67, 2006.
- [22] J. Zhou, J. Chen, and J. Ye. Malsar: Multi-task learning via structural regularization, 2012.
- [23] Y. Zhou, R. Jin, and S. C. Hoi. Exclusive lasso for multi-task feature selection. In *Proceedings of the International Conference on Artificial Intelligence and Statistics (AISTATS)*, 2010.

7 Appendix

7.1 Proofs of Lemmas and other Results

Here, we outline proofs of Lemmas and results that we deferred in the main paper. Before we prove the results, recall that we define

$$h(\mathbf{x}) = \inf_{\mathcal{W}} \sum_{G \in \mathcal{G}} (\alpha_G \|\mathbf{w}_G\| + \|\mathbf{w}_G\|_1) \quad \text{s.t.} \quad \sum_{G \in \mathcal{G}} \mathbf{w}_G = \mathbf{x}$$

As in the paper, we assume $\alpha_G = 1 \quad \forall G \in \mathcal{G}$.

7.1.1 Proof of Lemma 3.1

Proof It is trivial to show that $h(\mathbf{x}) \geq 0$ with equality iff $\mathbf{x} = 0$. We now show positive homogeneity. Suppose \mathbf{w}_G , $G \in \mathcal{G}$ is an optimal decomposition of \mathbf{x} , and let $\gamma \in \mathbb{R} \setminus \{0\}$. Then, $\sum_{G \in \mathcal{G}} \mathbf{w}_G = \mathbf{x} \Rightarrow \sum_{G \in \mathcal{G}} \gamma \mathbf{w}_G = \gamma \mathbf{x}$. This leads to the following set of inequalities:

$$h(\mathbf{x}) = \sum_{G \in \mathcal{G}} (\|\mathbf{w}_G\| + \|\mathbf{w}_G\|_1) = \frac{1}{|\gamma|} \sum_{G \in \mathcal{G}} (\|\gamma \mathbf{w}_G\| + \|\gamma \mathbf{w}_G\|_1) \geq \frac{1}{|\gamma|} h(\gamma \mathbf{x}) \quad (6)$$

Now, assuming \mathbf{v}_G , $G \in \mathcal{G}$ is an optimal decomposition of $\gamma \mathbf{x}$, we have that $\sum_{G \in \mathcal{G}} \frac{\mathbf{v}_G}{\gamma} = \mathbf{x}$, and we get

$$h(\gamma \mathbf{x}) = \sum_{G \in \mathcal{G}} (\|\mathbf{v}_G\| + \|\mathbf{v}_G\|_1) = |\gamma| \sum_{G \in \mathcal{G}} \left(\left\| \frac{\mathbf{v}_G}{\gamma} \right\| + \left\| \frac{\mathbf{v}_G}{\gamma} \right\|_1 \right) \geq |\gamma| h(\mathbf{x}) \quad (7)$$

Positive homogeneity follows from (6) and (7). The inequalities are a result of the possibility of the vectors not corresponding to the respective optimal decompositions.

For the triangle inequality, again let $\mathbf{w}_G, \mathbf{v}_G$ correspond to the optimal decomposition for \mathbf{x}, \mathbf{y} respectively. Then by definition,

$$\begin{aligned} h(\mathbf{x} + \mathbf{y}) &\leq \sum_{G \in \mathcal{G}} (\|\mathbf{w}_G + \mathbf{v}_G\| + \|\mathbf{w}_G + \mathbf{v}_G\|_1) \\ &\leq \sum_{G \in \mathcal{G}} (\|\mathbf{w}_G\| + \|\mathbf{v}_G\| + \|\mathbf{w}_G\|_1 + \|\mathbf{v}_G\|_1) \\ &= h(\mathbf{x}) + h(\mathbf{y}) \end{aligned}$$

The first and second inequalities follow by definition and the triangle inequality respectively. ■

7.1.2 Proof of Lemma 3.3

Proof Let $\mathbf{a} \in sA$ and $\mathbf{b} \in sB^\perp$ be two vectors. Let \mathbf{w}^A and \mathbf{w}^B correspond to the vectors in the optimal decompositions of \mathbf{a} and \mathbf{b} respectively. Note that $S \subset \bigcup_{G \in \mathcal{G}^*} G$. Since the vectors \mathbf{w}^A and \mathbf{w}^B are the optimal decompositions, we have that none of the supports of the vectors \mathbf{w}^A overlap with those in \mathbf{w}^B . Hence,

$$\begin{aligned} h(\mathbf{a}) + h(\mathbf{b}) &= \sum_{G \in \mathcal{G}^*} (\|\mathbf{w}_G^A\| + \|\mathbf{w}_G^A\|_1) + \sum_{G \in \mathcal{G}} (\|\mathbf{w}_G^B\| + \|\mathbf{w}_G^B\|_1) \\ &= \sum_{G \in \mathcal{G}} (\|\mathbf{w}_G^A\| + \|\mathbf{w}_G^B\| + \|\mathbf{w}_G^A\|_1 + \|\mathbf{w}_G^B\|_1) = h(\mathbf{a} + \mathbf{b}) \end{aligned}$$

This proves decomposability of $h(\cdot)$ over the subsets sA and sB . ■

7.2 More Motivation and Results for the Neuroscience Application

Analysis of fMRI data poses a number of computational and conceptual challenges. Healthy brains have much in common: anatomically, they have many of the same structures; functionally, there is rough correspondence among which structures underly which processes. Despite these high level commonalities, no two brains are identical, neither in their physical form nor their functional activity. Thus, to benefit from handling a multi-subject fMRI dataset as a multitask learning problem, a balance must be struck between similarity in macrostructure and dissimilarity in microstructure.

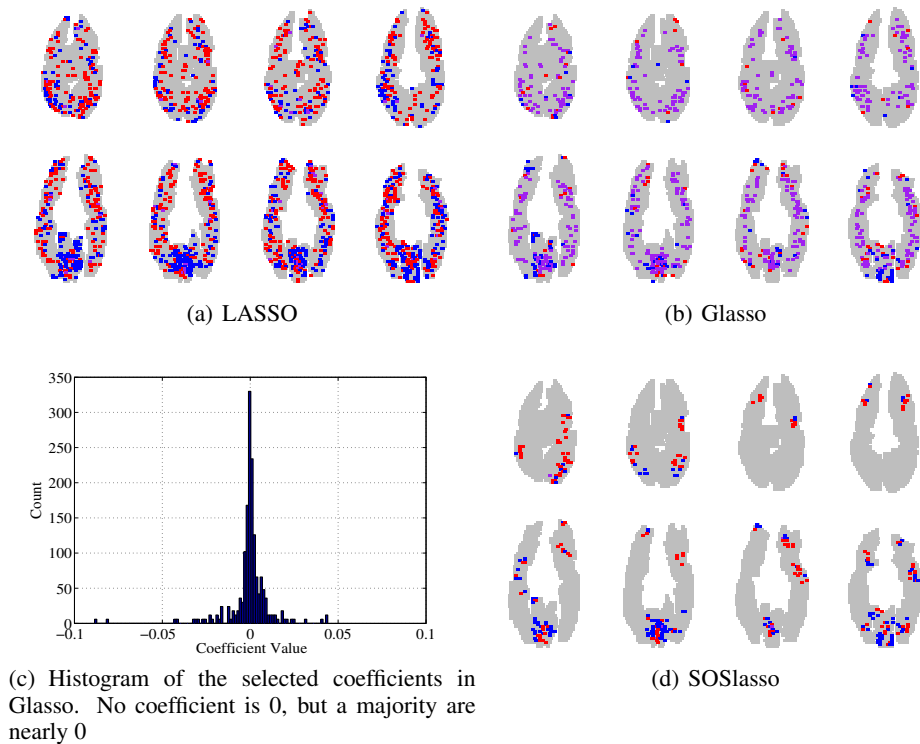


Figure 4: Per-slice result of the aggregated sparsity patterns across 6 subjects.

Standard multi-subject analysis involve voxel-wise “massively univariate” statistical methods that test explicitly, independently at each datapoint in space, if that point is responding in the same way to the presence of a stimulus. To align voxels somewhat across subjects, each subject’s data is co-registered to a common atlas, but because only crude alignment is possible, datasets are also typically spatially blurred so that large scale region level effects are emphasized at the expense of idiosyncratic patterns of activity at a finer scale. This approach has many weaknesses, such as it’s blindness to the multivariate relationships among voxels, its reliance on unattainable alignment, and subsequent spatial blurring that restricts analysis to very coarse descriptions of the signal—problematic because it is now well established that a great deal of information is carried within these local distributed patterns [5].

Multitask learning has the potential to address these problems, by leveraging information across subjects in some way while discovering multivariate solutions for each subject. However, if the method requires that an identical set of features be used in all solutions, as with standard group lasso (Glasso; [21]), then the same problems with alignment and non-correspondence of voxels across subjects are confronted. In the main paper, we demonstrate this issue.

Sparse group lasso [16] and our extension, sparse overlapping sets lasso, were motivated by these multitask challenges in which similar but not identical sets of features are likely important across tasks. SOSlasso addresses the problem by solving for a sparsity pattern over a set of arbitrarily defined and potentially overlapping groups, and then allowing unique solutions for each task that draw from this sparse common set of groups. A related solution to the same problem is proposed in [9].

7.2.1 Additional Experimental Results

We trained a classifier using 4-fold cross validation on the star plus dataset [20]. Figure 4 shows the discovered sparsity patterns in their entirety for the three methods considered, projected into a brain space that is the union over all size subjects; anatomical data was not available. In each slice, we aggregate the data for all the 6 subjects. Red points indicate voxels that contributed positively to picture classification in at least one subject, but never to sentences; Blue points have the opposite interpretation. Purple points indicate voxels that contributed positively to picture and sentence classification in different subjects.

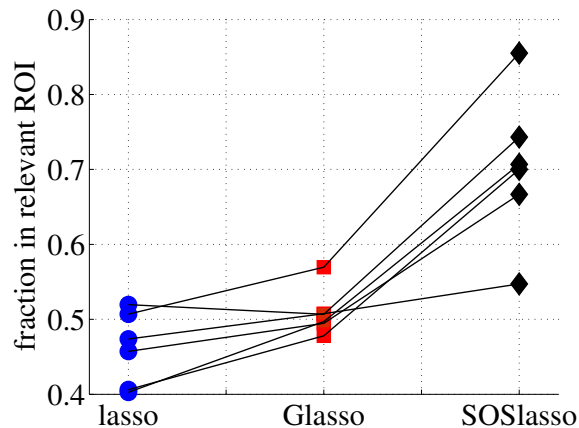


Figure 5: The proportion of discovered voxels that belong to the 7 pre-specified regions of each subject’s brain that neuroscientists expect to be especially involved with the current study. These 7 regions encompass 40% of the voxels of each subject, on average, and can be interpreted as chance.

The following observations are to be noted from Figure 4. The lasso solution (Figure 4(a)) results in a highly distributed sparsity pattern across individuals. This stems from the fact that the method does not explicitly take into account the similarities across brains of individuals, and hence does not look to “tie” the patterns together. Since the alignment is not perfect across brains, the 6 resulting patterns when aggregated result in a distributed pattern, and the largest error among the methods tested.

The Glasso (Figure 4(b)) for multitask learning ties a single voxel across 6 subjects into a single group. If a particular group is active, then all the coefficients in the group are active. Hence, if a particular voxel in a particular subject is selected, then the same (i, j, k) location in another subject will also be selected. This forced selection of voxels results in many coefficients that are almost but not exactly 0, and random signs as can be seen from the histogram of the selected voxels in Figure 4(c).

The lasso with Sparse Overlapping Sets (Figure 4(d)) overcomes the drawback of the Glasso by not forcing all the voxels at a particular location to be active. Also, since we consider $5 \times 5 \times 1$ groups here, we also tend to group voxels that are spatially clustered. This results in selecting voxels in a subject that are “close-by” (in a spatial sense) to voxels in other subjects. The result is a more clustered sparsity pattern compared to the lasso, and very few ambiguous voxels compared to the Glasso.

The mere fact that we specify groups of colocated voxels does not account for the fact that we discovered clear sparse-group structure. Indeed, we trained the latent group lasso [6] with the same group size ($5 \times 5 \times 1$ voxels) and absolutely no structure was recovered, and classification performance was near chance (45% error, relative to chance 50%). It fails because of its inflexibility with respect to the voxels within groups. If a group is selected, all the voxels contained must be utilized by all subjects. This forces many detrimental voxels into individual solutions, and leads to no group out performing any others. As a result, almost all groups are activated, and the feature selection effort fails. SOSlasso succeeds because it allows task-specific within group sparsity, and because, by allowing overlap, the set of groups is larger. This second factor reduces the chance that the informative regions of the brain are not well captured in any group.

An advantage of using this dataset is that each subject’s brain was been partitioned into 24 regions of interests, and expert neuroscientists identified 7 of these regions in particular that ought to be especially involved in processing the pictures and sentences in this study [20]. No one expects that every neural unit in these regions behave the same way, and that identical sets of these neural units will be involved in different subject’s brains as they complete the study. But it is reasonable to expect that there will be *similar* sparse sets voxels in these regions across subjects that are useful to classifying the kind of stimulus being viewed. Because the signal is sparse within subjects, and because spatially similar voxels may be more correlated than spatially dissimilar voxels, standard lasso without multitask learning will miss this structure; because not all voxels within these regions are relevant in all subjects, standard Glasso—even Glasso set up to explicitly handle the 24 regions of interests as groups—will do poorly at recovering the expected pattern of group sparsity. SOSlasso is expected to excel at recovering this pattern, and as we show in Figure 5 our method finds solutions with a high proportion of voxels in these 7 expected ROIs, far higher than the other methods considered.